FLAVOR SYMMETRY STUDIES WITH NEW HYPERON DATA FROM THE CRYSTAL BALL

B.M.K. NEFKENS, E. BERGER, S. MCDONALD N. PHAISANGITTISAKUL, J.W. PRICE, S. PRAKHOV, A. STAROSTIN, AND W.B. TIPPENS

UCLA, Los Angeles, CA 90095, USA

for the Crystal Ball Collaboration[*] [†]

New hyperon data produced in the reactions $K^-p \to neutrals$ have been measured using the Crystal Ball 4π multiphoton spectrometer. They provide striking evidence for the important role of flavor symmetry in QCD at low energy. We will show that the pronounced features seen in $\pi^-p \to \eta n$ near threshold are also exhibited in $K^-p \to \eta\Lambda$. The unique features of the $\pi^-p \to \pi^0\pi^0 n$ Dalitz plot are replicated in the flavor–symmetric reaction $K^-p \to \pi^0\pi^0\Lambda$, while $K^-p \to \pi^0\pi^0\Sigma^0$, which is not flavor–related, is much different. The measured mass, width, and spin/parity of the Λ^* octet hyperons are found to be the flavor symmetric copy of the N^* states. Flavor symmetry combined with the narrowness of Ξ^* states implies that searching for the missing baryon states may be done more profitably in the Ξ^* family rather than in the N^* or Δ^* family.

1 Introduction

Data on hyperon resonances are needed to evaluate the role of the approximate flavor symmetry of QCD in the non–perturbative regime. The QCD Lagrangian can be divided rather conveniently into two parts,

$$\mathcal{L}_{QCD} = \mathcal{L}_0 + \mathcal{L}_m, \tag{1}$$

$$\mathcal{L}_0 = -\frac{1}{4}F_{\mu\nu}F^{\mu\nu} + i\sum_q \overline{\psi}_q\gamma^\mu D_\mu\psi_q, \tag{2}$$

where the symbols are defined in the literature [1]. $\mathcal{L}_0$ depends on quark and gluon fields, their derivatives, and on one universal coupling constant. $\mathcal{L}_0$ has

---

[*]The Crystal Ball Collaboration: E. Berger, M. Clajus, A. Marušić, S. McDonald, B.M.K. Nefkens, N. Phaisangittisakul, S. Prakhov, M. Pulver, A. Starostin and W.B. Tippens, *UCLA*, D. Isenhower and M. Sadler, *ACU*, C. Allgower and H. Spinka, *ANL*, J. Comfort, K. Craig and T. Ramirez, *ASU*, T. Kycia, *BNL*, J. Peterson, *UCo*, W. Briscoe and A. Shafi, *GWU*, H.M. Staudenmaier, *UKa*, D.M. Manley and J. Olmsted, *KSU*, D. Peaslee, *UMd*, V. Bekrenev, A. Koulbardis, N. Kozlenko, S. Kruglov and I. Lopatin, *PNPI*, G.M. Huber, N. Knecht, G.J. Lolos and Z. Papandreou, *UReg*, I. Slaus and I. Supek, *RBI*, D.Grosnick, D. Koetke, R. Manweiler and S. Stanislaus, *ValU*.

[†]Supported by US DOE, NSF, NSEKC, RMS and US.

flavor symmetry, which means that the six quark flavors have identical strong interactions. This symmetry of $\mathcal{L}_0$ is broken by the mass term

$$\mathcal{L}_m = -\overline{\psi}_u m_u \psi_u - \overline{\psi}_d m_d \psi_d - \overline{\psi}_s m_s \psi_s - \cdots . \tag{3}$$

The characteristic hadronic energy scale is 1 GeV; this is much larger than the masses of the light quarks, $m_u \simeq 5$ MeV, $m_d \simeq 8$ MeV and $m_s \simeq 170$ MeV. We may therefore expect that flavor symmetry is only broken mildly and can be used profitably in reactions involving the light quarks u, d, and s. The flavor symmetry of the u and d quarks alone is known as isospin invariance. Its validity is well–established, not only in low energy nuclear physics but also in meson and baryon physics at medium and high energy [2]. Flavor symmetry of u, d, and s–quark systems is often explored as SU(3)–flavor symmetry. The breaking due to the mass term is more pronounced than for isospin. Various properties of the three light meson families and the six light baryon families are related by SU(3)–flavor symmetry with a correction for the breaking due to the different actual quark masses. For instance, we have the well–established Gell–Mann baryon–decuplet ground state and the Gell–Mann–Okubo baryon–octet ground state mass relations. There are also the relations among the baryon magnetic dipole moments obtained by naive quark models. We will investigate the use of flavor symmetry as it manifests itself in the dynamics of selected reactions. The unique features of η threshold production seen in $\pi^- p \to \eta n$ are duplicated in $K^- p \to \eta \Lambda$. Also, we have found that the Dalitz–plot characteristics of $\pi^- p \to \pi^0 \pi^0 n$ are replicated in $K^- p \to \pi^0 \pi^0 \Lambda$, but not in $K^- p \to \pi^0 \pi^0 \Sigma^0$ as anticipated by flavor symmetry.

New results on η, $2\pi^0$, π^0, γ and $\overline{K}^0$ production in $K^- p$ interactions up to $p_K = 760$ MeV/c have been obtained with the Crystal Ball (CB), a 4π multiphoton spectrometer. The CB was built and used originally at SLAC. It is now set up in a separated K^- beam of the AGS at Brookhaven National Laboratory. A 10 cm long liquid H_2 target has been installed in the center of the CB. The properties of the Crystal Ball (CB) multiphoton spectrometer have been discussed in this workshop by W. Briscoe. Details of the CB and data analysis are given in Refs. [3,4,5,6]. We have measured simultaneously all neutral final states in $K^- p$ interactions. We report here on the production of η and $2\pi^0$, and compare with our results from $\pi^- p$. In Sec. 4 we apply SU(3)–flavor symmetry to calculate the masses of the Λ^* resonances from the known N^* masses. In Sec. 5 we apply SU(3)–flavor to the search for the "missing" baryon resonances.

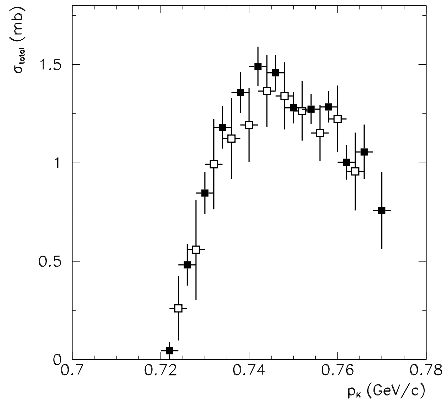

Figure 1. Preliminary CB results for $\sigma_t(K^- p \to \eta\Lambda)$ as function of p_{K^-}. The open squares are for the $\eta \to 3\pi^0$ and the solid squares for the $\eta \to 2\gamma$ decay mode.

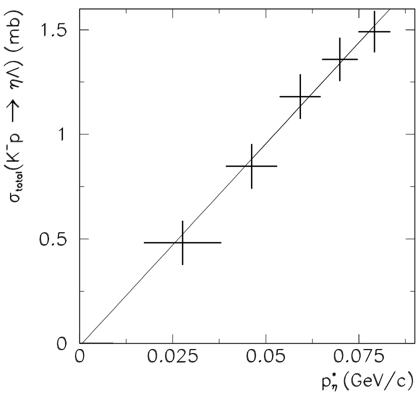

Figure 2. Preliminary $\sigma_t(K^- p \to \eta\Lambda)$ as function of p^*_η.

2 $K^- p \to \eta\Lambda$

The η decays 39% into 2γ and 32% into $3\pi^0 \to 6\gamma$, while 36% of Λ decay is to $\pi^0 n \to 2\gamma n$. We have measured the reaction $K^- p \to \eta\Lambda$ from the four photon cluster event sample when two clusters are due to $\eta \to 2\gamma$ and the other two to $\Lambda \to \pi^0 n \to 2\gamma n$; the neutron is not detected. We have also used eight cluster events detecting $\eta \to 3\pi^0 \to 6\gamma$ as well as $\Lambda \to \pi^0 n \to 2\gamma n$. Both event samples are very clean, and our two separate sets of results are in good agreement.

Shown in Fig. 1 is $\sigma_t(K^- p \to \eta\Lambda)$ as a function of the incident K^- momentum from threshold to 770 MeV/c. Note the steep onset of strong η production directly at threshold. In the interval from threshold at $p_K =$ 722 MeV/c to 740 MeV/c, the rise in σ_t is as expected for s–wave production (see Fig. 2). We find that

$$\sigma_t = C \times p^*_\eta, \tag{4}$$

where C is a constant, characteristic of s–wave production reactions, and p^*_η is the η c.m. momentum. Our data yield $C = (19 \pm 4)\mu\text{b}/(\text{MeV}/c)$.

The maximum of $\sigma_t(K^- p \to \eta\Lambda)$ is 1.5 ± 0.1 mb. It occurs at about $p_K = 740$ MeV/c. This is a large cross section, considering the phase space is small, p^*_η is merely 81 MeV/c. This should be compared to the $\bar{K}N$ final

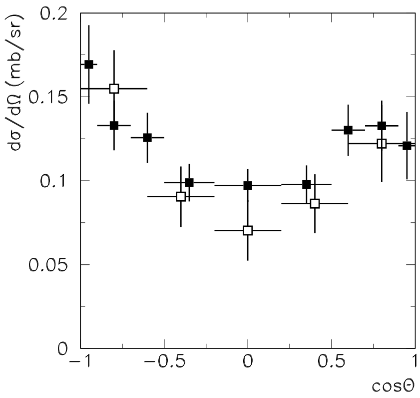

Figure 3. Preliminary $d\sigma(K^-p \to \eta\Lambda)$ at $p_{K^-} = 745\,\mathrm{MeV}/c$.

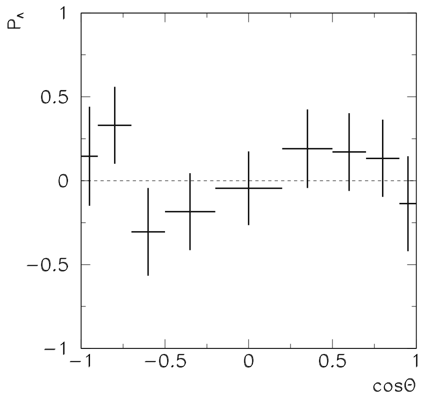

Figure 4. Preliminary Λ polarization in $K^-p \to \eta\Lambda$ at 735 MeV/c.

state, for which p^*_K is 414 MeV/c.

$d\sigma(K^-p \to \eta\Lambda)$ is shown in Fig. 3 The bowl shape is indicative of a *small* d–wave contribution. The polarization of the recoil Λ is displayed in Fig. 4. It is small, as expected when s–wave production is dominant.

The various features of η threshold production in $K^-p \to \eta\Lambda$, as displayed in Figs. 1–4, can be understood when we assume that η production is dominated by the excitation of the $\Lambda(1670)\frac{1}{2}^-$ resonance with a minimal contribution by other Λ^* states. It resembles in its various aspects the reaction $\pi^-p \to \eta n$. This includes:

1. The steep rise in σ_t at the opening of the η channel.

2. s–wave dominance with similar characteristic C–coefficients (see Eq. 4),

$$\sigma_t(K^-p \to \eta\Lambda) = (19 \pm 4)\,(\mu\mathrm{b}/(\mathrm{MeV}/c)) \times p^*_\eta$$
$$\sigma_t(\pi^-p \to \eta n) = (21 \pm 2)\,(\mu\mathrm{b}/(\mathrm{MeV}/c)) \times p^*_\eta \quad (5)$$

3. Large value for σ_t not far from the opening of the η channel; the maximum value for $\sigma_t(K^-p \to \eta\Lambda)$ is 1.5 ± 0.1 mb with $p^*_\eta = 81$ MeV/c, while for $\sigma_t(\pi^-p \to \eta n)$ the max is 2.6 ± 0.3 mb with $p^*_\eta = 182$ MeV/c [7].

4. The angular distribution somewhat above threshold has a bowl–like shape which may be described by a second order Legendre polynomial with similar coefficients for both $K^-p \to \eta\Lambda$ and $\pi^-p \to \eta n$. This is not a

trivial observation as η production by photons [8] or protons [9] has the opposite shape (it is dome–like).

We summarize as follows: η threshold production by K^- and π^- have the same features. This is a clear manifestation of the important role that approximate flavor symmetry plays in the dynamics of hadron interactions at intermediate energies. Furthermore, the two important intermediate state resonances, the $\Lambda(1670)\frac{1}{2}^-$ and the $N(1535)\frac{1}{2}^-$, belong to the same $SU(3)$ octet. This brings into question the proposal that the $N(1535)\frac{1}{2}^-$ may be mainly a $K\Sigma - K\Lambda$ bound state as proposed in Ref. [10] rather than a simple three quark state.

3 $\pi^- p \to \pi^0\pi^0 n$, $K^- p \to \pi^0\pi^0\Lambda$ and $K^- p \to \pi^0\pi^0\Sigma^0$

Another case which illustrates the permeating role of SU(3)–flavor symmetry is $2\pi^0$ production. Consider $\pi^- p \to \pi^0\pi^0 n$. The data are a byproduct of our investigations of rare η decay [4]. The Dalitz–plot (D–plot) at $p_\pi = 720$ MeV/c is shown in Fig. 5a. The $\pi^0\pi^0 n$ final state has two identical π^0's; we have taken this into account in Fig. 5a by double plotting each event, once for each π^0. The D–plot is dominated by a high concentration of events on an "island". There is only a faint indication of a vertical band structure which one naively would expect from a N^* or Δ^* intermediate state. There is no uniform horizontal density distribution that would signal the significant production of the f_0 (also called σ) s–wave dipion phenomenon. The projection of the D–plot distribution on the $m^2(\pi^0\pi^0)$ axis is shown in Fig. 5c together with the phase space; $m^2(\pi^0\pi^0)$ is the square of the $\pi^0\pi^0$ invariant mass. The $\pi^0\pi^0$ spectrum increases markedly with increasing $m(\pi^0\pi^0)$. Figure 5b represents the D–plot projection on the $m^2(\pi^0 n)$ axis. It has a towering peak at $m^2(\pi^0 n) = (1.2\ \mathrm{GeV})^2$, which is close to the mass of the $\Delta(1232)\frac{3}{2}^+$ resonance. The width of the peak is about 110 MeV, which is close to the Δ width. Our interpretation of Figs. 5a–5c is that $2\pi^0$ production here is dominated by the sequence $\pi^- p \to N^* \to \pi^0\Delta(1232)\frac{3}{2}^+ \to \pi^0\pi^0 n$. The p–wave decay of the Δ is likely responsible for the "island" feature of the D–plot. There is only a small contribution from $\pi^- p \to N^* \to f_0\ n \to \pi^0\pi^0 n$. At our incident π^- momentum of 720 MeV/c, the intermediate state N^* is a melange of $N(1440)\frac{1}{2}^+$, $N(1535)\frac{1}{2}^-$ and $N(1520)\frac{3}{2}^-$. The flavor analog processes of the ones just discussed are $K^- p \to \Lambda^* \to \pi^0\Sigma^0(1385)\frac{3}{2}^+ \to \pi^0\pi^0\Lambda$ and $K^- p \to \Lambda^* \to f_0\Lambda \to \pi^0\pi^0\Lambda$. Here, Λ^* is a medley of the $\Lambda(1600)\frac{1}{2}^+, \Lambda(1670)\frac{1}{2}^-$ and $\Lambda(1690)\frac{3}{2}^-$. Note that the $N(1440)\frac{1}{2}^+$ and $\Lambda(1660)\frac{1}{2}^+$ belong to the

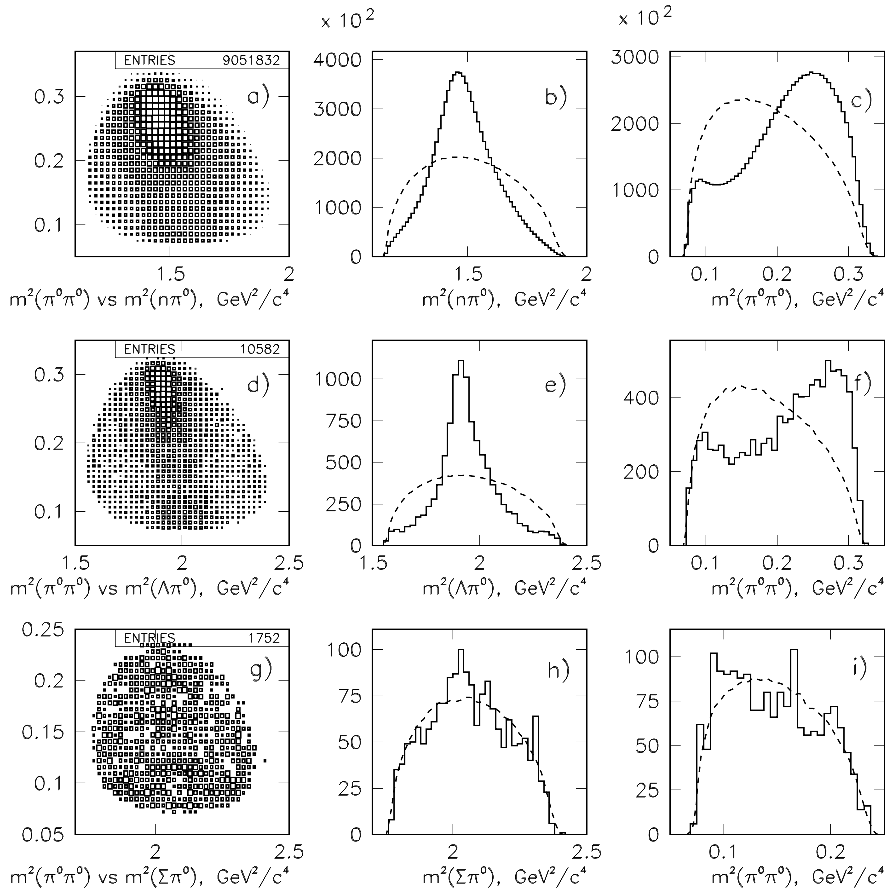

Figure 5. Figures a–c: $\pi^- p \to \pi^0\pi^0 n$ at $p_{\pi^-} = 720$ MeV/c; d–f: $K^- p \to \pi^0\pi^0\Lambda$ at $p_{K^-} = 750$ MeV/c; g–i: $K^- p \to \pi^0\pi^0\Sigma^0$ at $p_{K^-} = 750$ MeV/c. Preliminary data. The dashed lines show the phase space.

same SU(3) octet, similarly, the $N(1535)\frac{1}{2}^-$ and the $\Lambda(1670)\frac{1}{2}^-$, also the $N(1520)\frac{3}{2}^-$ and the $\Lambda(1690)\frac{3}{2}^-$ while the $\Delta(1232)\frac{3}{2}^+$ and $\Sigma(1385)\frac{3}{2}^+$ are part of the same SU(3) decuplet.

The CB results on $K^- p \to \pi^0\pi^0\Lambda$ at $p_{K^-} = 750$ MeV/c are shown in Figs. 5d–5c. They cover about the same $m(2\pi^0)$ region as $\pi^- p \to \pi^0\pi^0 n$ at 720 MeV/c. The resemblance of the outstanding features of Figs 5a–5c and

5d–5f is a clear illustration of the significant role played by flavor symmetry when dealing with the dynamics of 3–body processes. The minor dissimilarities originate in the difference in the width of the intermediate states; the $\Sigma(1385)\frac{3}{2}^+$ width is about half that of the $\Delta(1232)\frac{3}{2}^+$. The origin of the width difference was discussed earlier at this workshop by Dan Olof Riska who suggested it comes mainly from the availability of the u and d quarks, which yields a ratio of the Σ to Δ width of $(2/3)^2 = 4/9$.

We have found that the magnitude of $\sigma_t(K^-p \to \pi^0\pi^0\Lambda)$ is about half that of $\sigma_t(\pi^-p \to \pi^0\pi^0 n)$, which is not too different from the proportionality seen in η production by K^- and π^- as mentioned in the previous section.

We want to contrast the two $2\pi^0$ production reactions just discussed with $K^-p \to \Sigma^* \to \pi^0\pi^0\Sigma^0$. Here Σ^* stands for the $\Sigma(1660)\frac{1}{2}^+$, the $\Sigma(1670)\frac{3}{2}^-$ and possibly one or more states which are listed in the Review of Particle Properties [1] as questionable states and are not given in the Summary table. The decay of the Σ^* could involve an intermediate state, the $\Lambda(1405)\frac{1}{2}^-$, thus $K^-p \to \Sigma^* \to \pi^0\Lambda(1405)\frac{1}{2}^- \to \pi^0\pi^0\Sigma^0$, the $\Lambda(1405)$ is not a flavor analog of $\Sigma(1385)\frac{3}{2}^+$ and $\Delta(1232)\frac{3}{2}^+$ that dominate the $K^-p \to \pi^0\pi^0\Lambda$ and $\pi^-p \to \pi^0\pi^0 n$ reactions. The $\Lambda(1405)$ is the $J^P = \frac{1}{2}^-$ SU(3) singlet, which has a totally antisymmetric flavor state function. In contrast, the $\Sigma(1385)$ and $\Delta(1232)$ states are members of the $J^P = \frac{3}{2}^+$ decuplet, which requires a totally symmetric flavor state function. Flavor symmetry implies that $\Sigma^* \to f_0\Sigma^* \to \pi^0\pi^0\Sigma^0$ and $\Lambda^* \to f_0\Lambda \to \pi^0\pi^0\Lambda$ should have similar features, though there is a small kinematic difference because the Σ^0 is 77 MeV heavier than the Λ.

The CB results on $K^-p \to \pi^0\pi^0\Sigma^0$ at $p_K = 750$ MeV/c are shown in Fig. 5g–5i. Because of the greater Σ^0 mass, the $\pi^0\pi^0$ invariant mass region is smaller than the one of Figs. 5c or 5f. The D–plot of Fig. 5g does not have the "signature" island that characterizes Figs. 5a and 5d. But the near uniform horizontal density distribution seen in Fig. 5d is consistent with a healthy f_0 role in $K^-p \to \pi^0\pi^0\Sigma^0$. There is one unexpected feature, namely $m(\pi^0\pi^0)$ peaks at low m (see Fig. 5i). This needs to be investigated at other p_K. Our preliminary results indicate that the Σ^0 production is considerably smaller than Λ production: $\sigma_t(K^-p \to \pi^0\pi^0\Lambda) < \frac{1}{5}\,\sigma_t(K^-p \to \pi^0\pi^0\Sigma^0)$.

The above results on $2\pi^0$ production have interesting consequences for current efforts in nuclear physics to find f_0 modification in the nuclear medium [5] as suggested by several theorists. Our results indicate that the preferred case for this is K^- interactions leading to the $f_0\Sigma^0$ final state.

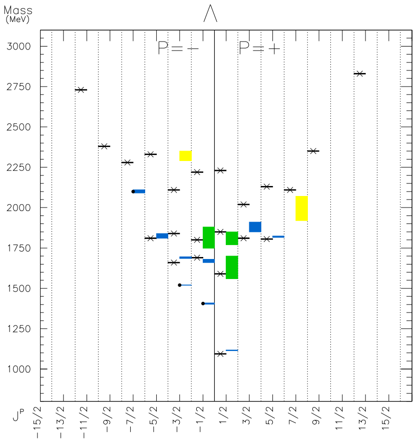

Figure 6. The spectrum of all Λ^* states arranged by spin, parity and mass. The boxes show the value of the mass and its uncertainty. Four–star resonances are shown with the darkest color, one–star with the lightest. The lines with the crosses are the predictions for all Λ^*–octet states. The Λ^*–singlet states are marked with a dots.

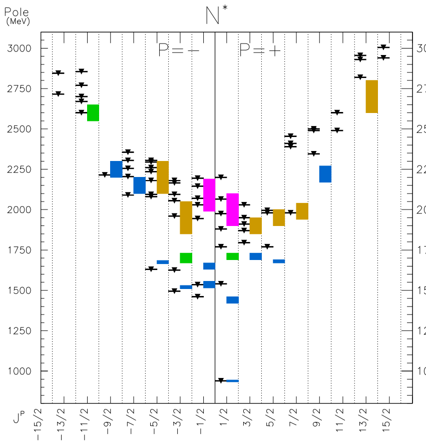

Figure 7. The spectrum of all N^* states arranged by spin, parity and pole positon. The boxes are the experimental pole positions [1]. Four–star resonances are shown with the darkest color, one–star with the lightest. The quark model prediction [12] are marked by the lines with dark triangles.

4 Flavor Symmetry and the Masses of the Hyperons

In the limit $\mathcal{L}_m \to 0$ the Λ^* octet states are the same as the N^* states, they have identical masses and spin/parities. When the finite quark masses are taken into consideration, the mass relation for flavor analog states is $m(\Lambda^*) = m(N^*) + \delta_m$. In lowest order, $\delta m = m_s - m_d \simeq 150$ MeV. This already accounts for all known octet Λ^* states to a level better than ~ 80 MeV. To obtain the next order correction, a model is needed such as the relativized constituent quark model [11]. Shown by shaded rectangular boxes in Fig. 6 are the masses of all Λ^*'s [1]. The states have been arranged according to spin and parity. The lines with crosses give our predictions for the masses of all octet Λ^* states, the input is the *experimental* N^* masses and δ_m as calculated from Ref. [11]. The agreement is spectacular.

5 Flavor Symmetry and the Search for the Missing Baryon Resonances

The known baryons in the various quark models are all (qqq) states and they obey approximate SU(3)–flavor symmetry. Quark models give a good account of the gross features of the observed baryons but fail in the details. Furthermore, most quark models predict the existence of many more states than have actually been observed. Proponents have dubbed the predicted but non–observed N^*'s the "missing" resonances. They allegedly have a very small coupling to the crucial πN–channel. It is also possible that the missing states are non-existing; the quark models could be incomplete because they do lack certain features such as a diquark substructure. There are efforts under way to find the missing states but with little success so far. Shown in Fig. 7 by shaded boxes are the known N^*'s, while the predicted ones by Capstick-Roberts [12] are indicated by a line with a triangle. In the mass region from 1850 to 2150 MeV there are 17 missing N^*'s: $3(\frac{1}{2}^+), 3(\frac{3}{2}^+), 1(\frac{5}{2}^+), 4(\frac{1}{2}^-), 4(\frac{3}{2}^-)$ and $2(\frac{5}{2}^-)$ states. Figure 8 shows the width of all known baryon resonances. In the region 1850–2150 MeV the N^* states are some 300 MeV wide; this fact greatly reduces the prospect of finding them. Note that the width of the known Ξ^* states is about 1/9 of the N^* or Δ^* width as expected from the Riska argument mentioned earlier. Flavor symmetry requires that for every missing N^* there should be a missing Ξ^* state that is about $3 \times (m_s - m_d) \simeq 450$ MeV heavier but with a narrow width, typically 30 MeV. To search for missing baryons, the Ξ^* family appears to have the edge. Such a search has been initiated at JLab [13].

6 Summary and Conclusion

New data on hyperon production obtained by the Crystal Ball collaboration have provided impressive manifestations of the large role played by approximate SU(3)–flavor symmetry. Specifically, we have shown the similarity in η threshold production by π^- and K^- as well as the similarity in $2\pi^0$ production, especially the sensitive Dalitz plot distribution in $\pi^- p \to \pi^0\pi^0 n$ and $K^- p \to \pi^0\pi^0\Lambda$ contrasting them with the very different $K^- p \to \pi^0\pi^0\Sigma^0$ Dalitz plot. Flavor symmetry explains the similarity of the octet Λ^* and N^* states, directly relating their masses and widths. Flavor symmetry considerations lead us to suggest to shift the search for missing baryons from the N^* and Δ^* to the Ξ^* family.

It is remarkable that baryon spectroscopy is rather successful without using directly a gluon degree of freedom. After all, the gluon plays an important

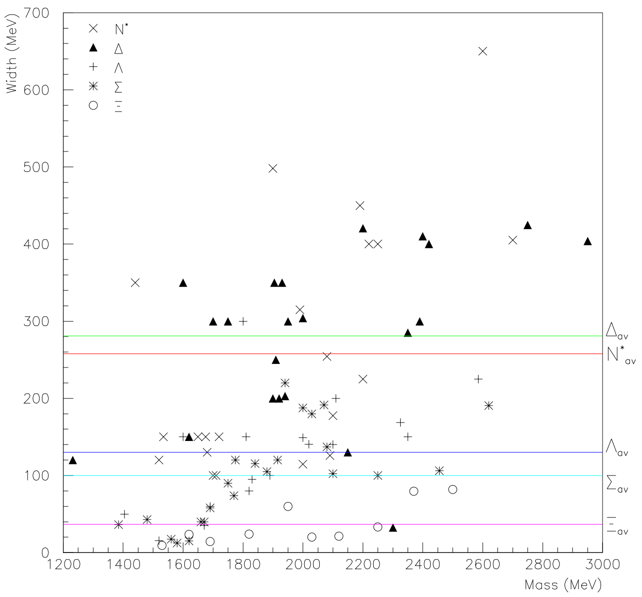

Figure 8. The width of all known baryon states.

role in the Lagrangian of QCD (see Eq. 1).

References

1. Particle Data Group, J. Eur. Physics. **C15** (2000).
2. G. Miller, B. Nefkens and I. Slaus, Phys. Rep.194, 1 (1990).
3. `http://bmkn8.physics.ucla.edu/Crystalball/crystalball.html`
4. S. Prakhov et al., Phys. Rev. Lett 84, 4802 (2000).
5. A. Starostin et al., Phys. Rev. Lett. 85,5539 (2000).
6. A. Starostin et al., submitted to Phys. Rev. C.
7. D. M. Binnie et al., Phys. Rev. D 8, 2789 (1973).
8. B. Krusche et al., Phys. Rev. Lett 74, 3736 (1995).
9. H. Calen et al., Phys. Lett. *B*458, 190 (1999).
10. N. Kaiser et al., Phys. Lett. *B*362, 23 (1995).
11. S. Capstick and N. Isgur, Phys. Rev. *D*34, 2809 (1986).
12. S. Capstick and W. Roberts, Phys. Rev. *D*49,4570 (1992).
13. J.W. Price, private communication.